

# Three Dimensional CFD Simulation Model with Experimental Validation of Silica Gel–Water Pair Adsorption Cooling Bed

AMIR A. ELGAMAL, TAHER HALAWA, HESHAM SAFWAT  
Mechanical Engineering Department,  
The British University in Egypt (BUE),  
El-Sherouk City, Cairo, 11837,  
EGYPT

*Abstract:* - In this paper, a three-dimensional full simulation model of a solar-driven adsorption cooling system integrated with user-defined functions (UDF) is successfully validated with a manufactured adsorption chamber filled with silica-gel type A. model is validated on the desorption phase with a maximum deviation error of 1.7%. Temperature with adsorption contours are shown for more understanding of the heat flow with adsorption behaviour inside the chamber in all directions. The maximum temperature at the desorption phase is reached after 300 seconds at fins area, and adsorption maximum uptake reached 0.16 kg/kg at fins wall but reached from 0.13 to 0.14 kg/kg around fins area. The average adsorption uptake reached 0.136 at the end of the adsorption process. The resultant uptake between adsorption and desorption is 0.018 kg/kg with a refrigerant mass of 1.8 kg in a complete cycle time.

*Key-Words:* - Energy, Solar, Adsorption, Cooling, Silica-gel, Simulation

Received: October 29, 2021. Revised: October 15, 2022. Accepted: November 17, 2022. Published: December 19, 2022.

## 1 Introduction

Energy and environment are the research topics that attract researchers to analyze and study. Waste heat, electricity, heating, and cooling are the main energy factors that affect energy consumption. The adsorption cycle is one of the solutions for all these kinds of energy sources, as it uses waste heat or solar heat to produce a cooling effect with a very low electrical consumption that could be used as a heat pump for heating and cooling. In addition to the low temperature required for regenerating silica gel below 100 °C, [1]. The adsorption cooling system is using adsorbents like silica gel with water to raise the pressure in the chamber, which is the main important part of the chiller, and like any other cooling system, a condenser is used then throttling in the evaporator to get the benefit of the cooling effect in the evaporator. In this study a silica gel–water pair is considered due to its high advantages over other working pairs like having a high uptake ratio, high latent heat of water, and being environmentally friendly. As shown in figure 1, the adsorption cycle contains two adsorbent beds, one in desorption heating mode and one in adsorption cooling mode. Beds are pressure-raising machines using an adsorption process in a constant volume bed. Adsorption and desorption processes in bed are one of the significant factors affecting COP (coefficient of performance) of the total process that

needs to be improved. Simulation in this field is done previously using FLUENT software and numerical simulation. Pan et al., [2], created a CFD model with 2D control volume for finned tube type and also simulated the passive and serial heat recoveries. Caglar., [3], simulated the effect of the number of fins and fin radius on the heat transfer and temperature, as the simulation is taken on a small 2D control volume domain using a CFD tool. Jribi et al., [4], simulated a 2D model for a small domain of an activated carbon-ethanol adsorption chamber, and simulation is validated with experimental results. Mohammed et al., [5], simulated a new compact heat exchanger bed design using a finite volume technique, and the simulation showed the effect of bed height, particle diameter, and vapour channel. Mohammadzadeh et al., [6], validated a numerical simulation model for a finned flat tube SWS-1L bed with experimental results and showed that COP is affected by fin height more than fin pitch. Geo et al., [7], simulated a chamber design with an annular adsorption bed, which is designed as the water vapour inlet coming from the annular direction inside a tube containing silica gel adsorbent and a water tube inside them. Results show improvements in the adsorption and reduced mass transfer resistance by increasing bed porosity inside the chamber. It is concluded that, from heat and mass transfer results, the importance of

reducing heat and mass transfer resistance, cooling method, and bed structure to increase bed performance. Ghilen et al., [8], simulated a two-bed adsorption chiller with mass recovery between two beds to reach pressure equilibrium, COP is raised to 0.7 while using a hot inlet temperature of 85 °C and 15 °C inlet evaporator temperature. Wang et al., [9], succeeded in validating a simulation model for two-bed adsorption chillers, and also studied the effect of cycle time on COP and SCP (specific cooling power) at different boundary conditions. Kurniawan et al., [10], simulated a finned tube adsorption bed to study the heat transfer parameters of adsorption and desorption processes. Moreover, the simulation showed the contours for adsorption on different locations of the bed and the weak points on the heat transfer and validated the simulation with an existing adsorption chiller system. Papakokkinos et al., [11], Created a general CFD for adsorption beds that is validated with experimental results, also simulation showed five different bed designs. Papakokkinos et al., [12], studied and simulated the hexagonal honeycomb heat exchanger design in an adsorption chamber. The cell in-radius of the heat exchanger affects the COP and SCP as the COP increases with the increase of the in-radius and reaches 0.606 for an in-radius of 6 mm and 0.356 for an in-radius of 1 mm. However, SCP is the opposite since it reached 80.4 W/Kgs for 6 mm in-radius and 218.9 W/Kgs for 1 mm in-radius. Fin thickness has almost no effect on the SCP, but the COP reached 0.599 at a fin thickness of 0.5 mm and 0.364 at a thickness of 3 mm. Fin length did not affect the COP but the SCP is 159.5 W/Kgs for a fin length of 5 mm and 86.1 W/Kgs for a fin length of 30 mm. Manila et al., [13], developed a computational model for a two-bed silica gel-water air cooled adsorption cooling system. The simulation evaluates the performance of a mesh between the shell and the heat exchanger containing adsorbent. Adsorption uptake enhanced with the mesh added to enhance the flow direction and minimise pressure drop for vapour flow. In addition, the optimum particle diameter used in this study is 0.4 mm as it shows the highest SCP and highest rate of adsorption, but it decreases the permeability of the flow and increases the pressure drop of the vapour. Based on the previous study, a full 3D model is not simulated with integrated UDFs. So, this paper aims to create a valid CFD 3D simulation model for an adsorption chamber in adsorption cooling systems with the integration of UDFs, as this model shows the adsorption behaviour and heat flow in all directions with more accurate results.

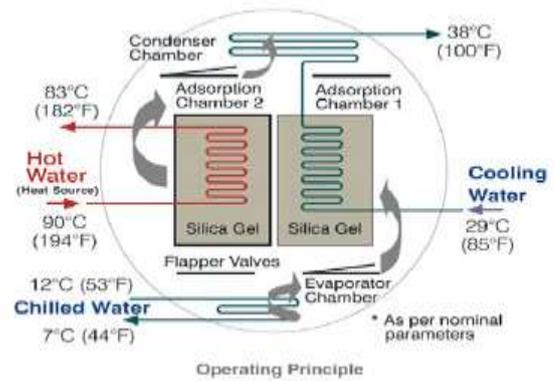


Fig. 1: Adsorption process scheme, retrieved from, [14].

## 2 Model Description

### 2.1 Experimental Setup

Chamber finned tube was designed and manufactured; it was used in the validation of the CFD study in this paper. Chamber is designed with a 9 mm fin pitch and 1 mm aluminium fin thickness. Chamber is connected to the condenser on the top and the evaporator to the bottom with a 1-inch diameter connection to reduce the pressure drop and connect a solenoid electric vapour valve. The chamber is filled with 10 kg of white silica gel type A, thermophysical properties of the three types of silica gel are listed in table 1. The tube arrangement is only one copper ½ inch tube with eight passes to increase the velocity of the fluid inside the tube to enhance the heat transfer coefficient. As shown in figure 3, the heating source is an electric heater with two different isolated tanks to ensure a constant temperature inlet over time, centrifugal pump is connected to the water heating system to ensure a constant flow rate during the experiment, volume flow rate sensor to measure the velocity of the fluid inside tubes with an accuracy of  $\pm 5\%$ , and three temperature sensors are installed to the inlet, outlet, and inside silica gel with an accuracy of  $\pm 0.3$  °C at the operating temperature of 63 °C. Figure 2 shows the chamber filled with silica gel before closing the cover with a gasket. Figure 4 shows the full adsorption chiller model design and manufactured chiller as the chamber is taken as a study point in this paper for the CFD validation.

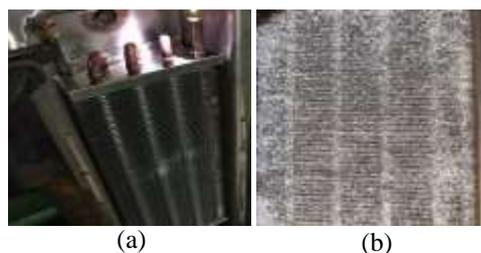


Fig. 2: Manufactured chamber (a) before filling (b) after filling with silica gel

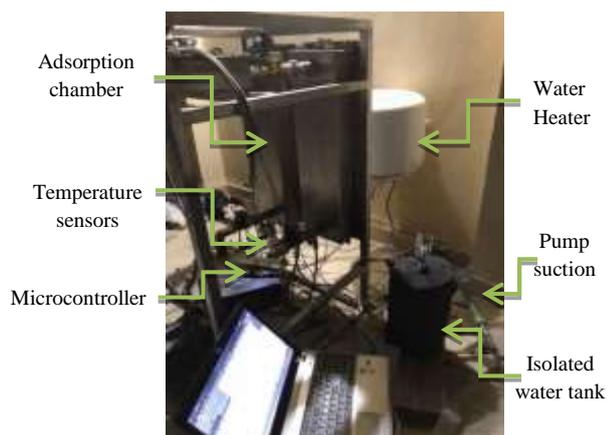


Fig. 3: Experimental setup

Table 1. Silica gel thermophysical properties, [14].

Property	Type A	Type 3A	Type RD
Specific surface area ( $m^2/g$ )	650	606	650
Porous volume (ml/g)	0.36	0.45	0.35
Average pore diameter (A)	22	30	21
Apparent density ( $kg/m^3$ )	730	770	800
pH value	5	3.9	4
Specific heat capacity ( $kJ/kg \cdot ^\circ k$ )	0.921	0.921	0.921
Thermal conductivity ( $W/m \cdot ^\circ k$ )	0.174	0.174	0.198

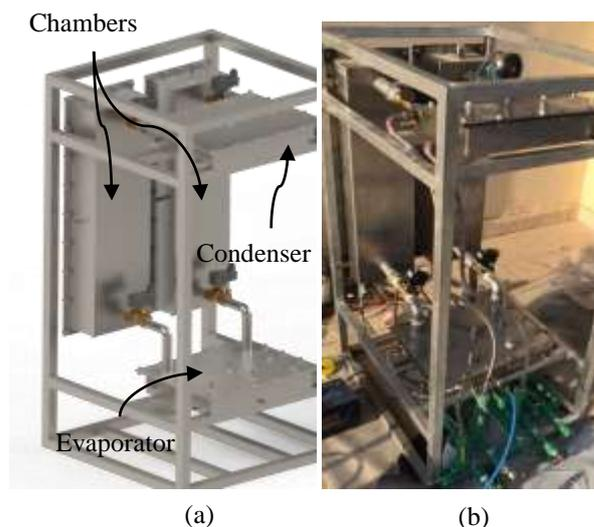


Fig. 4: Adsorption chiller setup (a) chiller design (b) manufactured chiller

## 2.2 CFD Model

### 2.2.1 Simulation Governing Equations

Desorption model validation with experimental setup will allow for more simulation studies on the desorption model with CFD governing Energy, mass, and Navier-Stokes equations on three dimensions.

The case is solved and integrated with a user-defined function of the heat source, mass source, momentum, and adsorption model over time with a transient simulation. Simulation assumptions are as follows.

- Silica gel particles have a uniform diameter and are equal to 1 mm as listed by the manufacturer specifications.
- Water vapour in the chamber is assumed to be an ideal gas.
- Water inside the tube is considered incompressible with constant density relative to its temperature.
- Porosity is assumed uniform based on the volume calculations of the chamber to the silica gel porous media.

Governing user-defined equations used in the simulation are as follows:

- Freundlich isotherm model.

This model suits the multilayer adsorption, and this is valid only for heterogeneous adsorption layers, [15].

$$X = X_{eq} \left( \frac{P_v}{P_s} \right)^{\frac{1}{n}} \quad (1)$$

Where  $X$  is the adsorption uptake ratio (kg adsorbate per kg adsorbent) and  $X_o$  is the maximum

uptake.  $(1/n)$  is the homogeneity of the surface and its value is between 0 and 1. This model is not valid for very high and low pressures, [15].

- Adsorption rate.

According to Emmanuel et al., [15], the rate of adsorption is defined by this expression,

$$\frac{dX}{dt} = K_m (X_o - X) \quad (2)$$

$$\frac{X - X_i}{X_{eq} - X_i} = 1 - e^{-K_m t} \quad (3)$$

Since silica gel is fully dried,

$$\frac{X}{X_{eq}} = 1 - e^{-K_m t} \quad (4)$$

Where  $K_m$  is the mass transfer coefficient, which is expressed by,

$$K_m = \frac{15D_s}{r_p^2} \quad (5)$$

$D_s$  is surface diffusivity and is given by,

$$D_s = D_{s0} e^{\frac{-E_a}{RT}} \quad (6)$$

$E_a$  is the activation energy, and  $D_{s0}$  is the pre-exponential term. All constants are listed in table 2.

- Mass source term.

Mass source term  $S_m$  describes the change in the adsorption concentration per time. It is negative in adsorption and positive in the desorption phase, [7].

$$S_m = \frac{\partial(\varepsilon_t \rho_g)}{\partial t} + \nabla(\rho_g \vec{u}) \quad (7)$$

source mass term can be expressed by the change in time as follows,

$$S_m = -(1 - \varepsilon_t) \rho_g \frac{\partial x}{\partial t} \quad (8)$$

- Saturation vapour pressure Equation

Saturated pressure of the water at a given temperature can be expressed by the following equation, [16].

$$P_s(T) = 0.0000888(T - 273.15)^3 - 0.0013802(T - 273.15)^2 + 0.0857427(T - 273.15) + 0.4709375 \quad (9)$$

- Energy Balance of the adsorber.

Adsorption heat energy source term represented by the following equation, [17].

$$\frac{\partial}{\partial t} [\varepsilon_b \rho_g E_g + (1 - \varepsilon_b) \rho_{ad} E_{ad}] + \nabla \cdot [\vec{v}(\rho_g E_g + P)] = \nabla \cdot (K_{eff} \vec{v} T) + \nabla \cdot (\underline{\tau} \cdot \vec{v}) + Q \quad (10)$$

Energy source term can be expressed by, [7],

$$Q = -\Delta H S_m \quad (11)$$

Where,  $Q$  is the energy source term in  $W/m^3$ ,  $\Delta H$  is the isosteric heat of adsorption in kJ/kg,  $\varepsilon_b$  is the bed porosity.

### 2.2.2 Simulation Model Details

The simulation model is chosen to be validated with the manufactured model to insure a valid model with as minimum simulation error as possible. The main problem with that model is the huge number of elements and computational time, so after validation, a reduced model needs to be validated with the original one with dimensional and heat transfer analysis. Dimensions of the full heat exchanger are given as shown in figure 5. Water flows inside tubes, copper tubes and aluminium fins between the water and silica gel domain on the outside. Silica gel domain is a water vapour fluid with silica gel porous media simulation model. Adsorption model and heat generation are added by user-defined functions and expressions using simulation governing equations listed above. Mesh independency test is done with 3.3 million elements which reached an acceptable accuracy and mesh quality with their different aspects. Governing equations are solved with a coupled pressure-based transient solver, using a k-epsilon realizable model. Workstation is used with two XEON 16 cores processors for this simulation and took 48 hours to simulate one minute.

The reduced model is chosen to be half of the full model that is validated with the experimental model, this is to ensure a valid flow in the chamber as the inlet is in the middle of the chamber side as shown in figure 6, and to also capture the effect of the fin length. In addition, this heat exchanger is only one tube with eight passes along the heat exchanger so this will affect the temperature and velocity distribution if a smaller model was taken. This reduced the number of elements to 1.8 million elements, and it reduced computational time without affecting the model's main values.

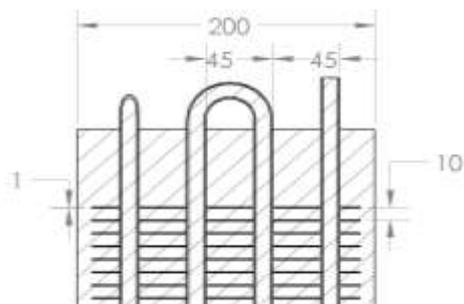


Fig. 5: Section drawing of the finned heat exchanger (all dimensions in mm)

Table 2. Values of the simulation model parameters

Parameter	Symbol	Value	Unit
Initial pressure	$P_i$	1000	kPa
Initial Chamber Temperature	$T_i$	20	°C
Total SG mass	$m_s$	10	kg
Hot Water inlet Temperature	$T_{hw,in}$	80	°C
Cooling water Temperature	$T_{cw,in}$	25	°C
Bed Porosity, [1].	$\epsilon_b$	0.37	—
Isosteric heat of adsorption, [15].	$\Delta H$	2560	kJ/kg
Pre-exponential term, [15].	$D_{s0}$	$2.54 \times 10^{-4}$	$m^2/s$
Activation Energy, [15].	$E_a$	$3.73 \times 10^4$	J/mol
Universal gas constant, [15].	R	8.314	J/mol · °K
Silica gel specific heat capacity, [15].	$C_{v,ad}$	924	J/kg · °K
Water specific heat, [18].	$C_{v,w}$	4180	J/kg · °K

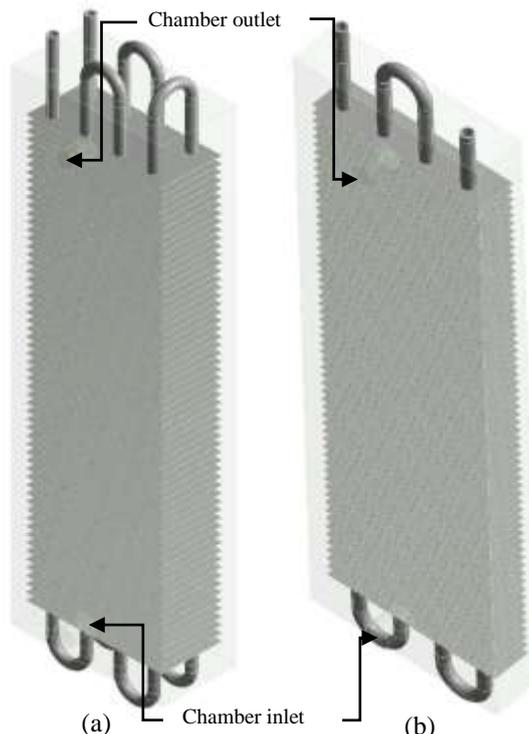


Fig. 6: Simulation geometry (a) Full model (b) Reduced model

### 3 Model Validation

In the experimental model section, a chamber manufactured in the adsorption chiller is tested in the desorption phase and validated with the full simulation model. Boundary conditions of the simulation are listed in table 3 as measured from the experimental data.

Figure 7 shows the difference between the full model in comparison with the experimental data.

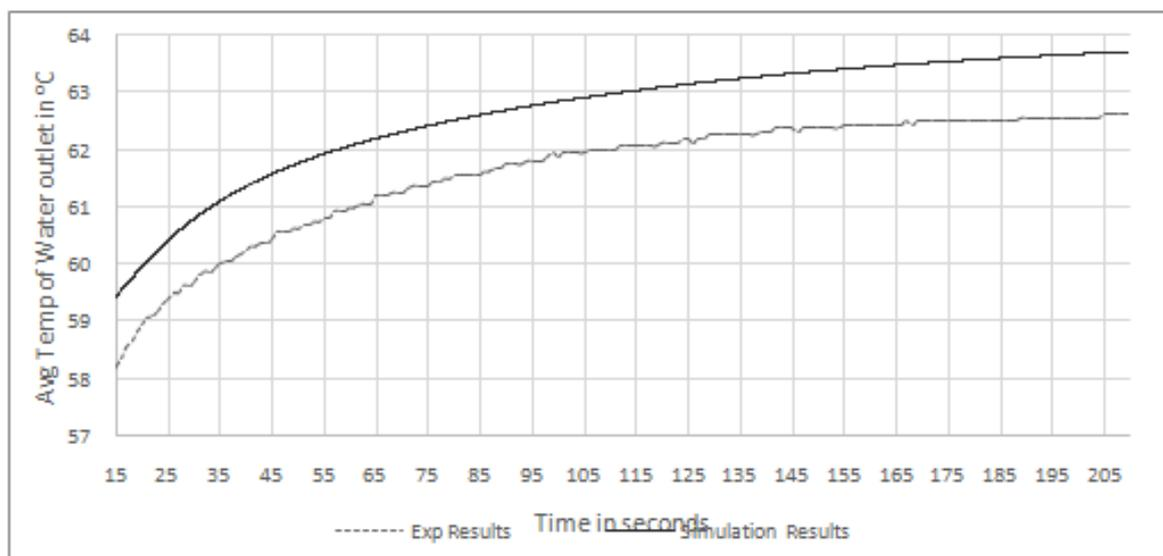


Fig. 7: Validation chart between experimental results and simulation results

Water temperature is decreasing at first seconds because of the initial values of the outlet temperature until the water comes out from the pipe outlet based on its velocity inside tubes in the full and reduced model. The temperature difference between the inlet and outlet is decreasing as the silica-gel temperature is increasing over time. This validation is acceptable and gives a maximum deviation of about 1.7 % between experimental and simulation results. The first 15 seconds are excluded from the simulation and experimental measurements to measure an accurate result from temperature sensors because water takes about 10 seconds to exit the heat exchanger with this velocity as the water is moving in only one pipe with multiple passes.

Simulation error is reduced by increasing the mesh quality and creating a finer mesh to reduce discretization error in the simulation model as known by the grid convergence test. In addition, residuals are reached  $10^{-6}$  in every time-step as the time-step value is reduced to 0.005 seconds after validating results with different time-step values to minimize the simulation error as possible.

Table 3. Simulation boundary conditions for validation

Parameter	Symbol	Value
Water inlet velocity	$V_{w,i}$	2.189 m/s
Initial chamber Temperature	$T_{b,i}$	20 °C
Initial Water Temperature	$T_{b,i}$	63.63 °C
Initial chamber pressure	$P_{b,i}$	1 kPa

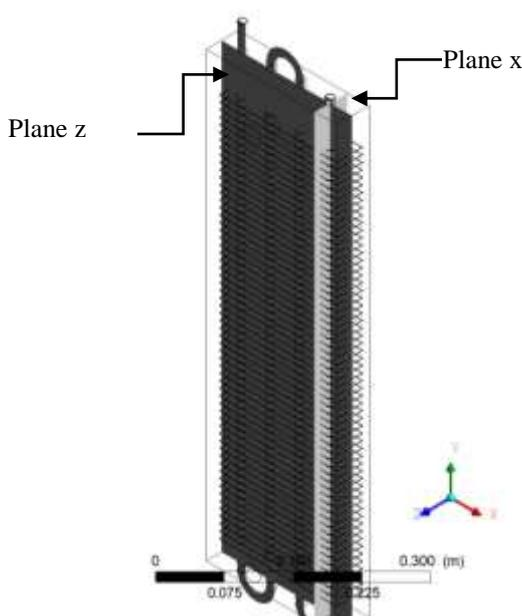


Fig. 8: Section planes used for presenting results

## 4 Results and Discussion

Adsorption chambers have 4 different processes, pre-heating, desorption, pre-cooling, and adsorption. Section planes x and z, as shown in figure 8, are taken to examine the effect of the heat exchanger and design parameters on the chamber at different heat directions.

### 4.1 Pre-heating and Heating (Desorption)

The pre-heating phase is the raise of the pressure period before opening the condenser valve to the chamber. Heating and preheating phases are the main source of water generation for the whole process, but this is not the main factor for the COP and SCP of the whole process as the adsorption uptake is much lower than desorption. 8 minutes cycle time of pre-heating and desorption as shown in figure 9 and figure 10, silica gel temperature is rising between fins area and reached almost maximum temperature after 300 seconds. As mentioned by Ng et al., [19], the type A silica gel takes 5 minutes to desorb 95% of the water content and 90 °C is sufficient to generate 95% of the water content. Heat flow in both directions is almost the same after 300 seconds with a temperature of about 36 °C at areas away from fins, however, this area is necessary for better vapour flow at the outlet and to make it easier to access the connections of the heat exchanger for maintenance. Moreover, temperature after 60 seconds only, can reach 60 °C in the fin area. Uptake at the end of the desorption process reached 0.117834.

### 4.2 Pre-cooling

As shown in figure 11 and figure 12, the pre-cooling contours, from 300 seconds to 480 seconds, temperature dropped from 80 °C to about 30 °C around fins. Moreover, after 3 minutes of cooling the maximum temperature recorded is about 42 °C at areas away slightly from fins. This is because of this area's high temperature in the last phase.

### 4.3 Adsorption

As the whole process performance depends on this phase, the adsorption contours are given from the user-defined functions with isotherm data given. As shown in the temperature contour in figure 13 and figure 14, temperature is increasing in areas away from fins, because of the adsorption temperature release during the adsorption phase reaching 38 °C in areas away from fins and 28 °C in areas around fins after the adsorption period. Figures also show the adsorption uptake at different times and the temperature effect on the adsorption as the highest

uptake reached 0.16 at the fins wall. Reducing fin spacing can help with the heat transfer hence the adsorption uptake in this phase.

#### 4.4 Overall Cycle Uptake Performance

Figure 15 shows the adsorbent temperature and uptake in a complete cycle time, temperature of the chamber in desorption reaches 63 °C after 5 minutes, and then in pre-cooling for 3 minutes, temperature reaches 34.5 °C. In adsorption process, temperature drop rate is decreased due to the isosteric heat of adsorption that is high at the beginning of the adsorption process according to the uptake ratio, temperature is decreasing as the cooling fluid inside the tubes cools the silica gel to obtain a higher adsorption uptake. Adsorption at a specific time that is a function in the saturation adsorption as mentioned in equation 2 based on the rate of adsorption, it reached an uptake of 0.136 kg/kg at 960 seconds which is the end of the adsorption process, so the net uptake during the whole cycle time is the difference between the uptake of the desorption phase and adsorption phase which is equal to 0.018 kg/kg. The rate of adsorption is also shown as the rate is high at the beginning of the adsorption process and decreases as the time increases, as it is affected by the temperature of the chamber. Refrigerant flow based on this net uptake is 1.8 kg of water per cycle time in one chamber.

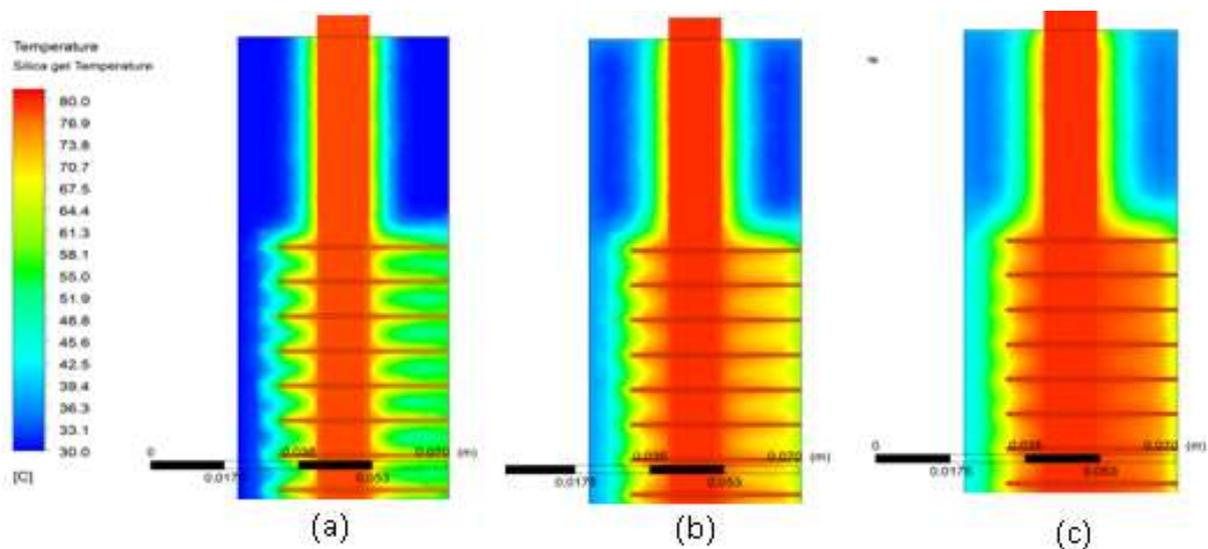


Fig. 9: Temperature contour of plane x in preheating and heating (a) 60 sec (b) 160 sec (c) 300 sec

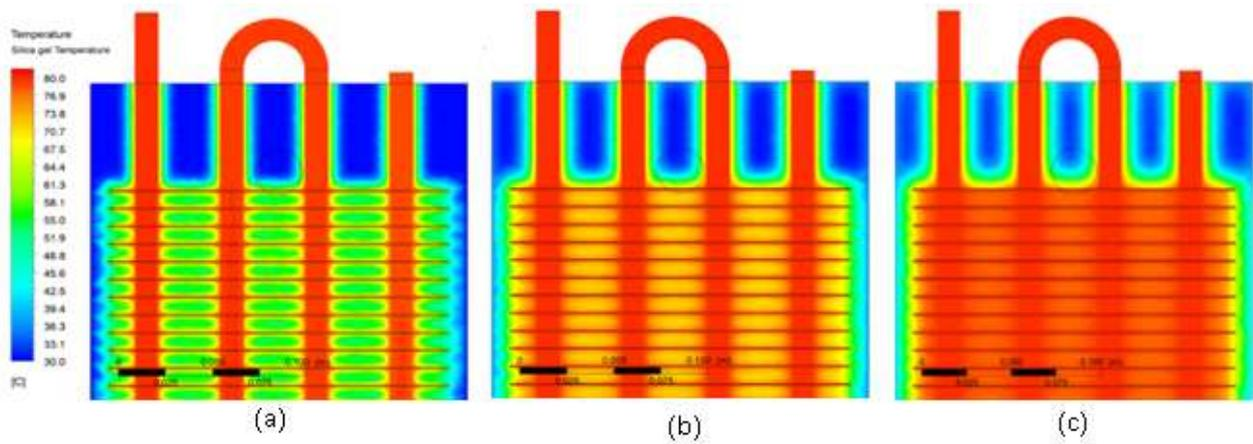


Fig. 10: Temperature contour of plane z in preheating and heating (a) 60 sec (b) 160 sec (c) 300 sec

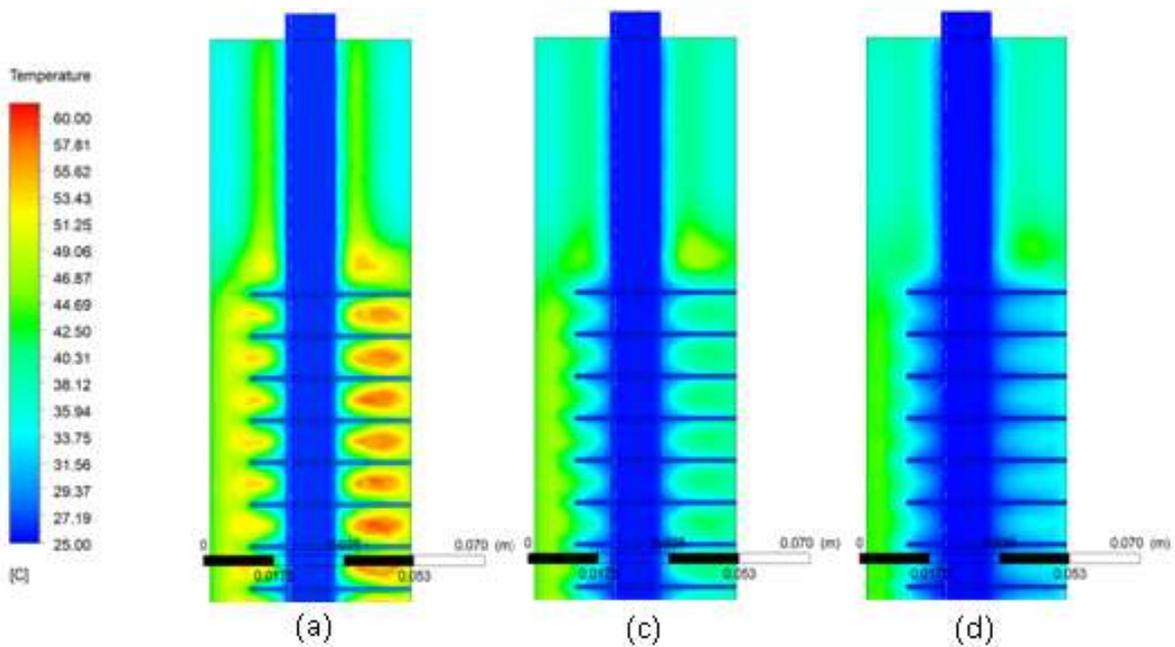


Fig. 11: Temperature contour of plane x in pre-cooling (a) 360 sec (b) 420 sec (c) 480 sec

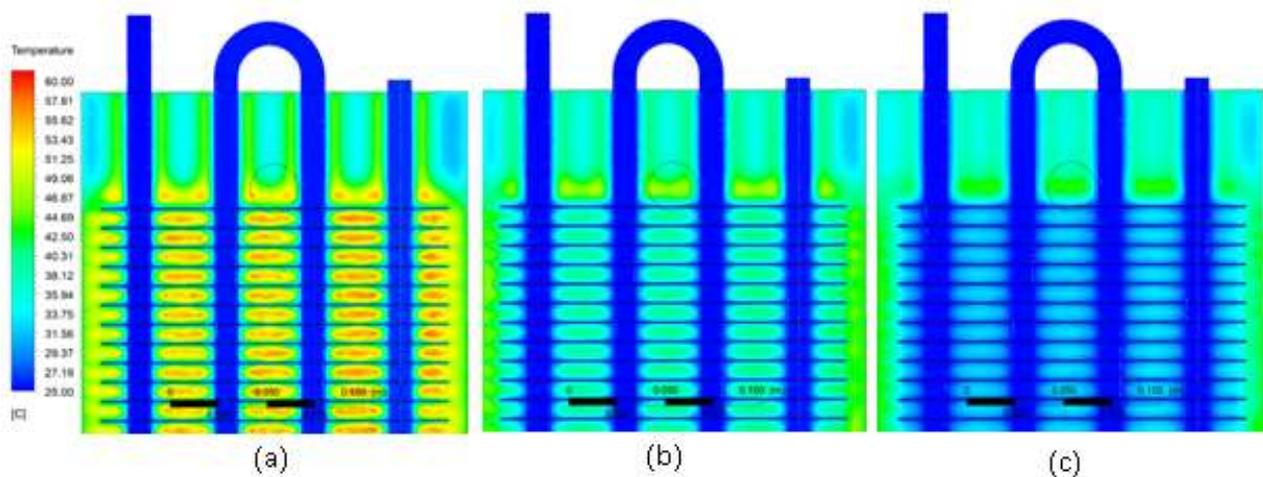


Fig. 12: Temperature contour of plane z in pre-cooling (a) 360 sec (b) 420 sec (c) 480 sec

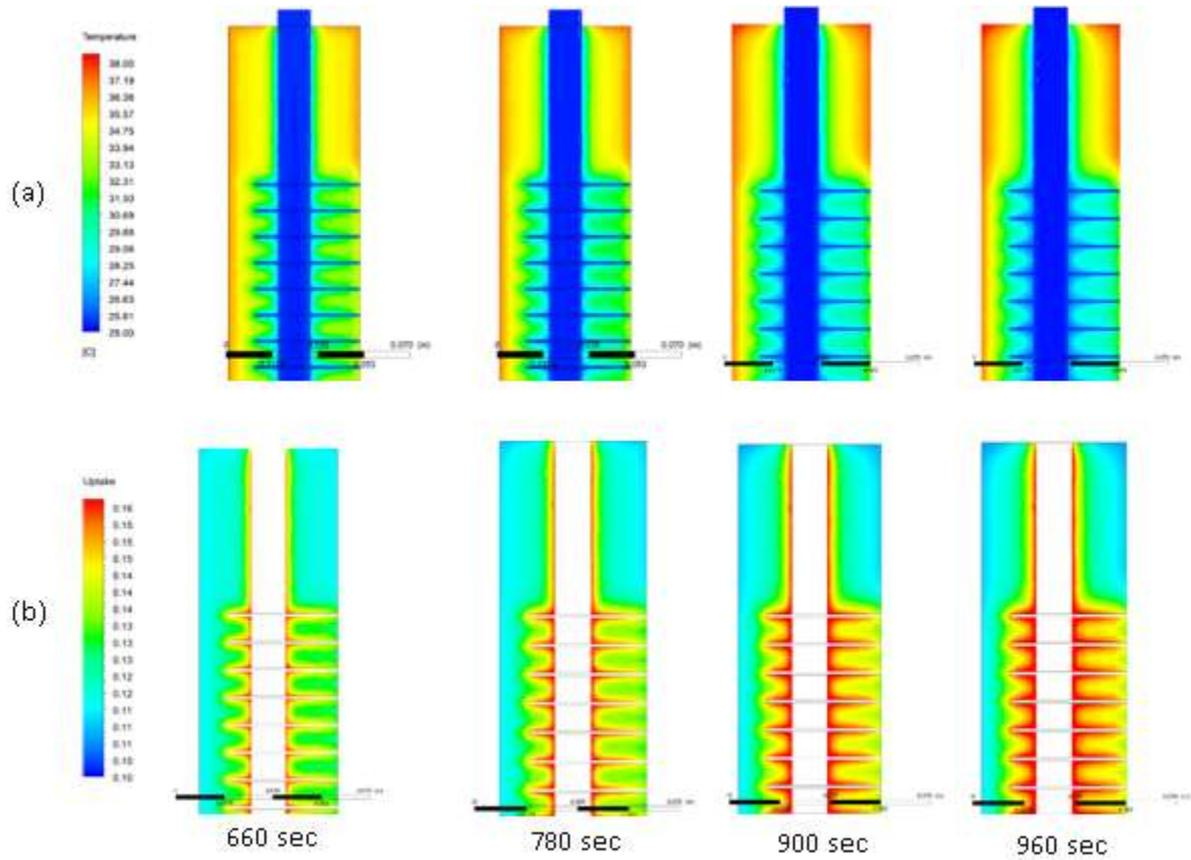


Fig. 13: plane x contours (a) Chamber and water temperature (b) Silica gel uptake

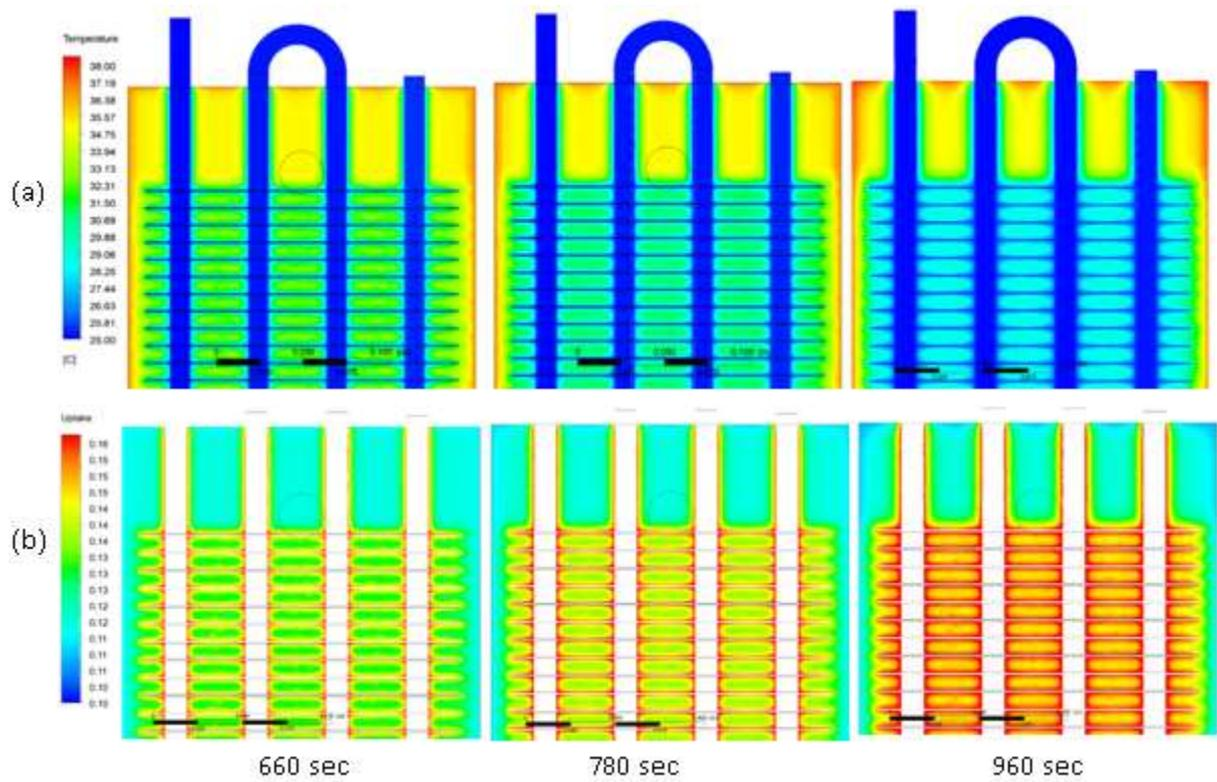


Fig. 14: plane z contours (a) Chamber and water temperature (b) Silica gel uptake

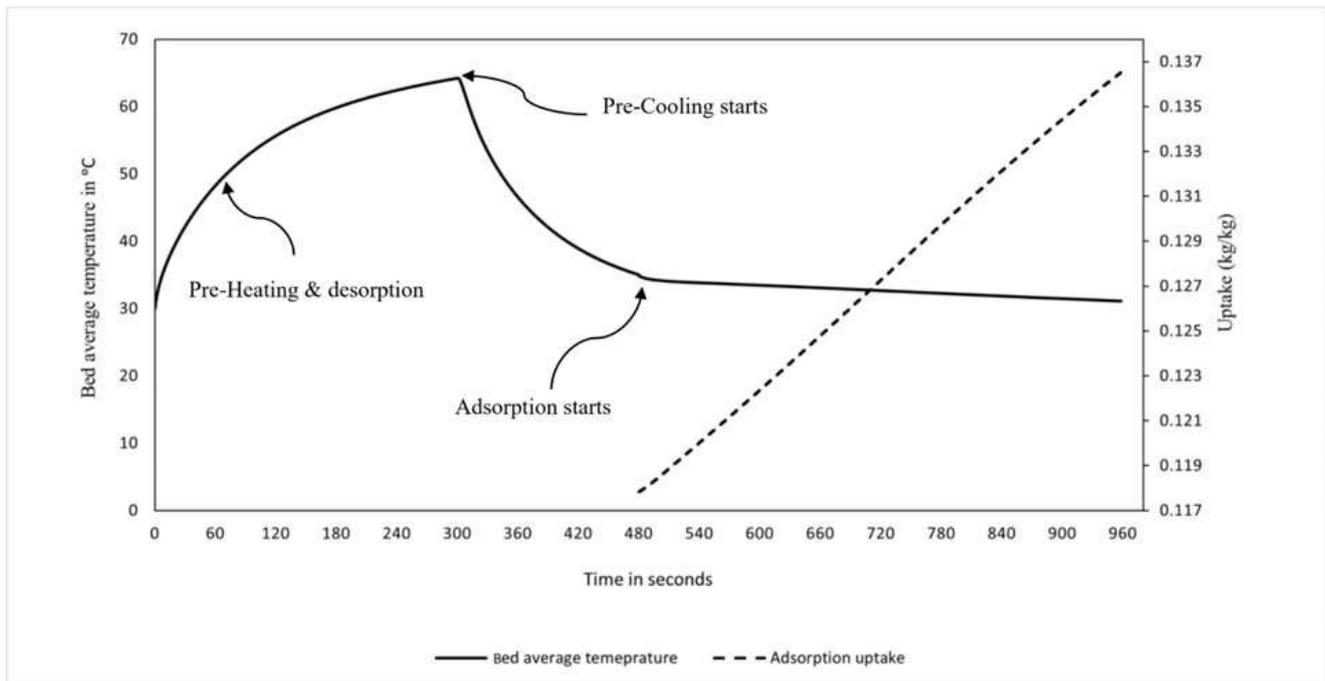


Fig. 15: Chamber average temperature and adsorption on time uptake for one complete cycle

## 5 Conclusion

The adsorption chamber is simulated and validated with a manufactured physical model. Cycle time of 8 minutes is chosen to simulate different phases of the adsorption chiller. Simulation results show the effect of heat exchanger dimensions and isotherm model integrated with mass source term and energy source term on the heat flow direction and uptake of the adsorbent under the operating conditions. Several conclusions were found:

- Temperature reached its maximum value around fins after 460 seconds.
- Pre-cooling period recorded a temperature of 40 °C around fins and a maximum of 50 °C away from fins.
- Adsorption is affected by the temperature of the silica gel and recorded uptake of 0.16 kg/kg around fins wall.
- Fin spacing needs to be reduced for higher adsorption uptake, but this needs more investigation to optimize the fin spacing with the silica gel amount at the same chamber volume.
- Adsorption phase uptake recorded 0.136 kg/kg, and the resultant uptake is 0.018 kg/kg which is equal to 1.8 kg of water refrigerant during the cycle time.
- Rate of adsorption is high at the beginning of the adsorption and decreases as adsorption time increases.

The success in validating a full 3D model of adsorption chamber can enhance the overall adsorption system in future studies by,

- Simulating the effect of the source heat temperature, cooling fluid temperature, evaporator inlet temperature, and cycle time.
- Simulating the effect of the heat exchanger parameters like fin spacing, tube diameter, and fin thickness on COP and SCP.
- Studying the effect of different isotherm models on the simulation with another validation study for the isotherm model.
- Simulating the effect of radiation on the chamber and its effect on the overall cycle performance.

### References:

- [1] H. T. Chua, K. C. Ng, W. Wang, C. Yap, and X. L. Wang, "Transient modeling of a two-bed silica gel-water adsorption chiller", doi: 10.1016/j.ijheatmasstransfer.2003.08.010.
- [2] Q. W. Pan, R. Z. Wang, and L. W. Wang, "Comparison of different kinds of heat recoveries applied in adsorption refrigeration system," *International Journal of Refrigeration*, vol. 55, pp. 37–48, 2015, doi: 10.1016/j.ijrefrig.2015.03.022.
- [3] A. Çağlar, "The effect of fin design parameters on the heat transfer enhancement in the adsorbent bed of a thermal wave cycle," *Appl Therm Eng*, vol. 104, pp. 386–393, 2016, doi: 10.1016/j.applthermaleng.2016.05.092.

- [4] S. Jribi, T. Miyazaki, B. B. Saha, S. Koyama, S. Maeda, and T. Maruyama, "Simulation par la mécanique numérique des fluides (CFD) et validation expérimentale de l'adsorption de l'éthanol sur un échangeur de chaleur compact à charbon actif," *International Journal of Refrigeration*, vol. 74, pp. 343–351, 2017, doi: 10.1016/j.ijrefrig.2016.10.019.
- [5] R. H. Mohammed, O. Mesalhy, and M. L. Elsayed, "Novel compact bed design for adsorption cooling systems: Parametric numerical study Conception d'un nouveau lit compact pour systèmes de refroidissement à adsorption: étude numérique paramétrique," *International Journal of Refrigeration*, vol. 80, pp. 238–251, 2017, doi: 10.1016/j.ijrefrig.2017.04.028.
- [6] M. Mohammadzadeh Kowsari, H. Niazmand, and M. M. Tokarev, "Bed configuration effects on the finned flat-tube adsorption heat exchanger performance: Numerical modeling and experimental validation," *Appl Energy*, vol. 213, no. July 2017, pp. 540–554, 2018, doi: 10.1016/j.apenergy.2017.11.019.
- [7] D. D. Gao, Y. X. Li, Z. X. Yuan, and S. W. Du, "Coupled heat and mass transfer in annular adsorption bed," 2016.
- [8] N. Ghilen, S. Gabsi, R. Benelmir, and M. el Ganaoui, "Performance Simulation of Two-Bed Adsorption Refrigeration Chiller with Mass Recovery," *Journal of Fundamentals of Renewable Energy and Applications*, vol. 7, no. 03, p. 3, 2017, doi: 10.4172/2090-4541.1000229i.
- [9] X. Lin Wang *et al.*, "Simulation of the Silica Gel-Water Adsorption Chillers SIMULATION OF SILICA GEL-WATER ADSORPTION CHILLERS," 2004. [Online]. Available: [http://docs.lib.purdue.edu/iracc/663TelNo.:](http://docs.lib.purdue.edu/iracc/663TelNo.)
- [10] A. Kurniawan, Nasruddin, and A. Rachmat, "CFD Simulation of Silica Gel as an Adsorbent on Finned Tube Adsorbent Bed," in *E3S Web of Conferences*, Nov. 2018, vol. 67. doi: 10.1051/e3sconf/20186701014.
- [11] G. Papakokkinos, J. Castro, J. López, and A. Oliva, "A generalized computational model for the simulation of adsorption packed bed reactors – Parametric study of five reactor geometries for cooling applications," *Appl Energy*, vol. 235, no. November 2018, pp. 409–427, 2019, doi: 10.1016/j.apenergy.2018.10.081.
- [12] G. Papakokkinos, J. Castro, C. Oliet, and A. Oliva, "Computational investigation of the hexagonal honeycomb adsorption reactor for cooling applications: Honeycomb adsorption reactor for cooling," *Appl Therm Eng*, vol. 202, no. November 2021, p. 117807, 2022, doi: 10.1016/j.applthermaleng.2021.117807.
- [13] M. R. Manila, S. Mitra, and P. Dutta, "Studies on dynamics of two-stage air cooled water/silica gel adsorption system," *Appl Therm Eng*, vol. 178, no. December 2019, p. 115552, 2020, doi: 10.1016/j.applthermaleng.2020.115552.
- [14] W. Yaïci and E. Entchev, "Coupled unsteady computational fluid dynamics with heat and mass transfer analysis of a solar/heat-powered adsorption cooling system for use in buildings," *Int J Heat Mass Transf*, vol. 144, p. 118648, Dec. 2019, doi: 10.1016/J.IJHEATMASSTRANSFER.2019.118648.
- [15] E. N. Ayisi and K. Fraña, "The Design and Test for Degradation of Energy Density of a Silica Gel-Based Energy Storage System Using Low Grade Heat for Desorption Phase," *Energies (Basel)*, vol. 13, no. 17, 2020, doi: 10.3390/en13174513.
- [16] G. Zhang, D. C. Wang, J. P. Zhang, Y. P. Han, and W. Sun, "Simulation of operating characteristics of the silica gel-water adsorption chiller powered by solar energy," *Solar Energy*, vol. 85, no. 7, pp. 1469–1478, Jul. 2011, doi: 10.1016/j.solener.2011.04.005.
- [17] ANSYS, "FLUENT 12.0 user's guide," 2013.
- [18] Cengel, *Heat and Mass Transfer: A Practical Approach*. Blacklick, Ohio, U.S.A.: McGraw-Hill Science Engineering, 2006.
- [19] K. C. Ng *et al.*, "Experimental investigation of the silica gel–water adsorption isotherm characteristics," *Appl Therm Eng*, vol. 21, no. 16, pp. 1631–1642, Nov. 2001, doi: 10.1016/S1359-4311(01)00039-4.

### Contribution of Individual Authors to the Creation of a Scientific Article (Ghostwriting Policy)

-Amir A. Elgamal carried out the simulation and numerical model, got the idea of the simulation, and wrote the research article.

-Taher Halawa got the idea of the simulation model, revised the paper, and supervised the numerical study.

-Hesham Safwat has organized and supervised the paper.

### Creative Commons Attribution License 4.0 (Attribution 4.0 International, CC BY 4.0)

This article is published under the terms of the Creative Commons Attribution License 4.0

[https://creativecommons.org/licenses/by/4.0/deed.en\\_US](https://creativecommons.org/licenses/by/4.0/deed.en_US)